Paper 13

HEAT TRANSFER MEASUREMENTS USING THIN FILM GAUGES

S.M. Guo, M.C. Spencer, G.D. Lock, T.V. Jones
University of Oxford
England

N.W. Harwey
Rolls-Royce plc
England

12th Symposium on Measuring Techniques for Transonic and Supersonic Flow in Cascades and Turbomachines, Prague, 12-13 September, 1994

Heat Transfer Measurements Using Thin Film Gauges

S. M. Guo, M. C. Spencer, G. D. Lock and T. V. Jones

Department of Engineering Science
Oxford University, England

N. W. Harvey

Rolls-Royce plc
Derby, England

Abstract

Thin film surface resistance thermometers have been used to measure the heat transfer to an annular turbine nozzle guide vane (NGV) in the Oxford University Cold Heat Transfer Tunnel [1]. Engine-representative Mach and Reynolds numbers were employed and the free-stream turbulence intensity was 13%. The NGVs were either precooled or preheated to create a range of different thermal boundary conditions. The gauges were mounted on both perspex and aluminium NGVs. The heat transfer coefficient was obtained from the surface temperature history using either a single layer analysis (for perspex) or double layer (for aluminium) analysis [2,3]. The surface temperature and heat transfer levels were also measured using rough and polished liquid crystals under similar conditions.

Introduction

Changes in the resistance of thin film metal layers can be related to their temperature. When placed on a substrate of known thermal properties, measurements of the temperature history of such metal films, coupled with the appropriate analytical model, can lead to the calculation of the surface heat flux history [2,3].

The use of such gauges for measuring heat transfer rates to turbine blades in short-duration transient cascade facilities is well documented [2,4]. As well as measuring the surface heat transfer rates, the interpretation of these signals can yield much useful information about the gas flow and boundary layers.

There are three general types of surface thin film gauges. The first type are mounted on a substrate which is considered semi-infinite [2]. A typical example of this type would be a thin film nickel or platinum resistance thermometer fired onto a macor, quartz or glass substrate. A second type are layered gauges where a thin insulating layer such as vitreous enamel, kapton or upilex is adhesively bonded to a model (usually made of metal) which has different thermal properties [5]. A upilex layer can also be mounted on perspex and because the thermal properties of both materials are similar, such a layered gauge can be considered semi-infinite. A third type of gauge is two-layered [6] where the temperature difference across a thermal resistance of accurately known properties and dimensions is measured.

Thin film gauges described in this paper are operated in a constant current mode. In this mode of operation, a small, constant sensing current is passed through the thin film in order to generate a change in voltage proportional to the change of film resistance and temperature. Thin film gauges can also be operated in a constant temperature mode where the thin film forms one arm of a Wheatstone bridge and feedback is used to keep the gauge resistance, and hence the temperature, constant. The output voltage is used to measure the electrical heating of the gauge.

Thin Film Gauges

The Osney Laboratory at Oxford [7] has developed a facility which specialises in manufacturing large arrays of thin films. A detailed description of the manufacturing process is available in laboratory reports [8,9]. A brief description is presented here.

The thin film gauges are fabricated from 0.04 μm thick pure platinum. The platinum is sputtered on to thin (50 μm) sheets of upilex. The sheet is then covered in a thin (0.5 μm) layer of copper using sputtering and evaporation techniques. Under darkened conditions, aerosol photoresist is sprayed over the surface. This surface is later exposed to UV light under a mask which leaves a pattern with the desired geometry of the leads after developing and etching. The dimensions of the gauges used are 0.1 by 2.0 mm (see figure 1) which give an adequate resolution for present purposes. Typically the gauge and lead resistances are 50 and 1 Ω respectively.

The flexible sheet of upilex is then wrapped around and glued to either perspex or aluminium NGVs. A typical set of thin films on a perspex NGV is shown in figure 2a and 2b. There are 11 gauges on the pressure surface and 15 gauges on the suction surface, all aligned on a streamline along midspan. Gauges have also been mounted at 10 and 90% span.

As discussed above, the surface temperature (T) is obtained by recording the resistance history of each gauge. The temperature is related to the resistance using $R = R_0(1 + \alpha(T - 20))$, where R_0 is the resistance at 20 C and α is the temperature coefficient of resistance. The value of α is obtained from calibration in a hot water bath and is typically ~ 0.001 K^{-1}.

Test Facility and Instrumentation

The measurements were performed in the Oxford University Cold Heat Transfer Tunnel [1,10], or CHTT. The test section of the tunnel is an annular cascade of 36 NGVs at 1.4 times larger than engine scale. The test duration of the facility (about 7 seconds at engine design conditions) enables transient techniques to be employed. The tunnel allows an independent variation of Reynolds and Mach numbers, or equivalently the upstream and downstream pressures can be independently and continuously varied. Details of the NGV geometry are given in table 1.

Table 1: **NGV Details**

Mid-span axial chord	0.0664 m
Mean pitch at exit	0.09718 m
Span at exit	0.08076 m
Turning angle	73°
Throat area	0.08056 m^2
Mean blade diameter	1.113 m

A schematic diagram of the CHTT is shown in figure 3. The operation of the tunnel is controlled by pneumatically-activated ball valves. Air flows from the high pressure reservoir (31 m^3 at 3 MPa) into a regulator system from which part of the flow enters an ejector. The remainder passes into the annular test section containing the NGVs, subsequently exhausting to atmosphere. Large levels of turbulence are created using a resistance plate with an open area of 9%. The turbulence intensity and length scale were measured using a hot-wire anemometer and found to be 13% and 21 mm at the NGV inlet plane.

For the experiments reported here, five NGVs and hub and tip end walls were preheated or precooled before running the tunnel by isolating four passages of the annulus with a purposely designed shutter mechanism and cassette [1,10] as illustrated in figure 4. The central NGV in the cassette was instrumented either with the thin film gauges or coated with narrow-band liquid crystals. A detailed description of the application of the transient liquid crystal technique to the CHTT is provided in reference [10] and only the instrumentation for thin film gauge measurements will be discussed here.

An constant current source was used to power eight thin film gauges. The current was minimised (< 1 mA) to avoid significant heating of the thin films. The voltage history of these gauges were amplified and then recorded at 2 kHz using an analogue to digital converter (CIO-AD16JR-AT) and a 386 pc. Higher frequency information can be obtained (on fewer channels) up to a rate of 300 kHz. Surface temperature histories were also recorded using two thermocouples on the NGV surface and a third thermocouple is used to measure the free-stream air temperature.

Data Reduction

The voltage history from the gauges leads to measurements of the change in the gauge resistance with time. From the temperature-resistance calibration a measurement of the surface temperature history is obtained. Both perspex and aluminium NGVs were used. The thermal properties of the upilex sheet are

very similar to those of perspex but significantly different from those of the metal. Consequently, different data reduction theories were used for the two materials. For the perspex blade, the substrate of the upilex, glue and perspex was considered to be a single, homogeneous material. The thin films on the upilex sheet with the metal blade was considered to be a layered gauge, with the upilex and glue a homogeneous material.

Perspex NGV

For the perspex NGV, the model insulating substrate (figure 1) is considered semi-infinite, i.e., for the times of interest heat conduction does not lower the inner temperature by an appreciable amount, and the one-dimensional heat conduction equation

$$\frac{\partial^2 T}{\partial x^2} = \frac{1}{\beta}\frac{\partial T}{\partial t} \tag{1}$$

may be solved for the heat transfer rate $\dot{q}$ at the surface. The boundary conditions for $\dot{q}(x,t)$ and $T(x,t)$ are $\dot{q}(0,t) = -k\partial T/\partial x$, $T(\infty,t) = T_0$, and $T(x,0) = T_0$. In the above equations T is the temperature, T_0 is the initial temperature, t the time, x the dimension normal to the surface, and β and k are the thermal diffusivity and thermal conductivity of the substrate. The time variation of $\dot{q}$ is evaluated from the surface temperature history using the Laplace transform method described in [2], viz.,

$$\dot{q}(t) = \dot{q}(m\tau) = 2\sqrt{\frac{\rho c k}{\pi\tau}}\sum_{n=0}^{m}(T_{n+1} + T_{n-1} - 2T_n)(m-n)^{0.5}\,, \tag{2}$$

where τ is the time interval between data points.

Metal NGV

For the metal blade a layered model must be used to calculate the heat transfer rate from the surface temperature history. Two different methods were used. The first assumes that the metal blade appears infinitely thick to the thermal waves propagating from the surface, i.e., the aluminium is semi-infinite. This method is accurate over most of the NGV surface but not in the trailing edge region where the thickness of the blade is as thin as 1 mm. A second method, using a numerical technique, has been used to account for the finite thickness of the metal in this region.

For the case of a semi-infinite backwall there is a thermally insulating layer ($i = 1, 0 < x < a$) and the metal substrate ($i = 2, a < x < \infty$), where a is the thickness of the upilex and glue. The governing equation is

$$\frac{\partial^2 T_i}{\partial x^2} = \frac{1}{\beta_i}\frac{\partial T_i}{\partial t},\ i = 1, 2 \tag{3}$$

with the boundary conditions $\dot{q} = -k\partial T_1/\partial x$ at $x = 0$, $T_1 = T_2$ at $x = a$, $-k_1\partial T_1/\partial x = -k_2\partial T_2/\partial x$ at $x = a$ and $\partial T_2/\partial x = 0$ at $x = \infty$. A solution to these equations, using Laplace Transforms, is presented in reference [3]. Solving for $\overline{T_1}$ and $\overline{T_2}$ yields,

$$\overline{T_1} = \frac{\dot{q}_s}{k_1}\sqrt{\frac{\beta_1}{s}}\left(\frac{(1+\sigma)\exp(-(x-a)\sqrt{s/\beta_1}) + (1-\sigma)\exp((x-a)\sqrt{s/\beta_1})}{(1+\sigma)\exp(a\sqrt{s/\beta_1}) - (1-\sigma)\exp(-a\sqrt{s/\beta_1})}\right) \tag{4}$$

$$\overline{T_2} = \frac{2\dot{q}_s}{k_1}\sqrt{\frac{\beta_1}{s}}\left(\frac{\exp((x-a)\sqrt{s/\beta_2})}{(1+\sigma)\exp(a\sqrt{s/\beta_1}) - (1-\sigma)\exp(-a\sqrt{s/\beta_1})}\right) \tag{5}$$

where $\sigma = \sqrt{(\rho_2 c_2 k_2)/(\rho_1 c_1 k_1)}$, $\dot{q}_s$ is the heat flux at $x = 0$, ρ and c are the substrate density and specific heat capacity, and s is the Laplace transform variable.

For the case of a finite depth metal substrate, the model has a thermally insulating layer ($i = 1, 0 < x < a$) of upilex and glue, and a metal substrate ($i = 2, a < x < b$) of finite dimension $b - a$. For this case, equation (3) is solved with the same boundary conditions as immediately above except that $\partial T_2/\partial x = 0$ at $x = b$, not at $x = \infty$. A solution for this case has been obtained [3] but a finite difference technique [11] was preferred here. This numerical technique is described in detail by Guo [9]. It should be noted that the finite depth analysis method was only required near the trailing edge of the blade and that calculations using this method were in agreement with the semi-infinite backwall method in all other regions.

Results and Discussion

All of the results presented here are at engine design conditions (Re = 1.95×10^6 and $M_{exit} = 0.96$) and with a free-stream turbulence intensity of 13% at NGV inlet. A typical surface temperature history

from a gauge on the pressure surface of a preheated ($T_0 \sim 60$ C) perspex NGV is shown in figure 5a. The CHTT begins operation at 3 s and, with the shutters lowered, a small amount of cold air leaks into the cassette until the shutters open (opening time 60 ms) at 4.6 s. The surface temperature is seen to drop until the tunnel is shut off at 7 s and then rises as the surface is reheated from the substrate. The heat transfer rate, calculated from equation (2), is shown as a function of time in figure 5b.

Figure 5c is a plot of the heat transfer coefficient (h) as a function of time. This is calculated from

$$h = \frac{\dot{q}}{T_s - T_g} \tag{6}$$

where T_s is the surface temperature and T_g is the local gas recovery temperature [12] defined by $T_g = T_\infty(1 + r(\gamma - 1)M_\infty^2/2)$ with T_∞ and M_∞ being the local gas temperature and Mach number, and $r = 0.87$ is the recovery factor. The total temperature history at inlet to the CHTT is shown in figure 5d and the local recovery temperature is calculated using the Mach number distribution around the NGV [10]. Note that h is at a constant level during the 2.5 s that the gauge encounters the steady flow.

The heat transfer coefficient measured by all gauges, each averaged over the steady portion of the run, is plotted against fraction of surface distance along the 10, 50 and 90% span streamlines in figure 6. This figure shows that along the midspan h falls from a stagnation level of 650 W/m^{2}K to a minimum of 350 W/m^{2}K at about 25% surface distance on the pressure surface. The heat transfer coefficient then rises to approximately 800 W/m^{2}K at the trailing edge. On the suction surface, transition is seen to occur at about 45% surface distance. The turbulent level of h is about 650 W/m^{2}K.

The heat transfer levels on the pressure surface do not vary greatly with different span positions. On the suction surface the highest levels of heat transfer occur at 90% span. At about 60% surface distance the heat transfer level along the 90% spanline drops significantly and dips below the midspan level at the trailing edge. This decrease in heat transfer level occurs in a region influenced by secondary flows. This region of separated flow on the suction surface has been identified using flow visualisation with coloured oil as shown in figure 7. The reduction in the heat transfer level is not as obvious at 10% span where, due to the radial pressure gradient, the separation lines do not extend as far from the hub end wall.

Another plot of heat transfer coefficient (W/m^{2}K) versus fraction of surface distance along the midspan streamline is shown in figure 8. This data was acquired over a range of thermal boundary conditions and different directions of heat flux. Various symbols appear in this figure and represent data taken from preheated ($T_0 \sim 60$ C), precooled ($T_0 \sim -15$ C), or ambient ($T_0 \sim 20$ C) conditions, and from either perspex or aluminium NGVs. The local gas recovery temperature used in the calculation of the heat transfer coefficient varied between 5 and 18 C around the NGV midspan. The data indicates that measurements using the aluminium and perspex materials yield the same heat transfer coefficient despite different analysis techniques. The measurements also show that the heat transfer coefficient is independent of whether the heat transfer is in a forward or reverse sense. This confirms that the Nusselt numbers obtained from measurements in the CHTT in a reverse heat transfer mode (hot blade, cool gas) [10] can be meaningfully related to the engine case (cool blade, hot gas).

Figures 9-11 compare the thin film gauge heat transfer measurements with those made using the transient liquid crystal technique [10]. The data from the liquid crystals exhibit similar features to those obtained using the thin film gauges, including the reduction in heat transfer coefficient in the regions influenced by secondary flow. The differences in the heat transfer levels are due to surface roughness. Different scales of roughness can be obtained by polishing the liquid crystals on the model surface. Unpolished crystals have a roughness (k) of ~ 25 μm and a second set of experiments were performed with semi-polished crystals with a roughness of ~ 10 μm. These figures show that the roughness increases the heat transfer to the pressure surface and alters the transition point on the suction surface despite the large levels of free-stream turbulence. These observations are similar to those found by Turner et al. [13]. It should be noted that liquid crystals can be polished down to a very smooth surface for studies of transition phenomena [14] but this was not pursued in the work presented here.

The value of y^+ (or roughness Reynolds number) [15],

$$\mathrm{Re}_k = y^+ = \frac{k u_\tau}{\nu} = \frac{k u_\infty \sqrt{c_f/2}}{\nu}$$

has been calculated for different positions along the pressure and suction surfaces and is shown in figure 12. In the above equation k is the roughness dimension, c_f is the skin friction coefficient, u_τ and u_∞ are

the local shear velocity and free-stream velocity at NGV exit, and ν is the viscosity. These calculations are an approximation based on a flat plate turbulent boundary layer and have been made in order to estimate whether the roughness of the unpolished and semi-polished liquid crystals on the NGV is likely to effect the heat transfer levels. A value of $Re_k < 5$ is considered to be hydraulically smooth and a value of $Re_k > 70$ is considered to be fully rough. In between the surface is considered to be transitionally rough. Figure 12 indicates that the semi-polished surface is transitionally rough at every point and this roughness is likely to effect both the heat transfer levels and the location of the transition point.

Conclusions

Thin film gauges have been successfully used to measure the heat transfer in an annular cascade of NGVs at engine-representative Reynolds and Mach numbers and high levels of free stream turbulence. Different analysis techniques were employed and the measurements made over a range of thermal boundary conditions. Conclusions can be drawn that for the case of high turbulence flow, thermal boundary layers are of little significance whereas surface roughness plays an important role.

Acknowledgements

The authors are grateful for the assistance of T. Godfrey, Z. Wang and P. Ireland. This work was funded by Rolls-Royce plc.

References

[1] Martinez-Botas, R. F., Main, A. J., Lock, G. D., and Jones, T. V., 1993, *A Cold Heat Transfer Tunnel For Gas Turbine Research on an Annular Cascade,* ASME 93-GT-248.

[2] Schultz, D. L., and Jones, T. V., 1973, *Heat Transfer Measurements in Short-Duration Hypersonic Facilities,* AGARD AG-165.

[3] Doorly, J. E. and Oldfield, M. L G., 1987, *The Theory of Advanced Multi-Layer Thin Film Heat Transfer Gauges,* Int. J. Heat Mass Transfer, (30), 6, 1159-1168.

[4] Oldfield, M. L. G., Jones, T. V., and Schultz, D. L., 1978, *On-Line Computer for Transient Turbine Cascade Instrumentation,* IEEE Transactions on Aerospace and Electronic Systems, AES-14, 5.

[5] Doorly, J. E. and Oldfield, M. L G., 1986, *New Heat Transfer Gauges for use on Multi-layered Substrates,* ASME J. Turbomachinery, (108), 1.

[6] Epstein, A. H., Guenette, G. R., Norton, R. J. G., and Cao Yuzhang, 1985, *High Frequency Response Heat Flux Gauges for Metal Blading,* AGARD-CP-390, Norway.

[7] Jones, T. V., 1988, *Gas Turbine Studies at Oxford 1969–1987,* ASME 88-GT-112.

[8] Hofeldt, A., 1993, *Thin Film Techniques and Turbulent Spot Studies,* First Year Report, Oxford University.

[9] Guo, S. M., 1994, *Thin Film Instrumentation on Plastic Substrates and Applications to Aerodynamics,* First Year Report, Oxford University.

[10] Martinez-Botas, R. F., Lock, G. D., and Jones, T. V., 1994, *Heat Transfer Measurements in an Annular Cascade of Transonic Gas Turbine Blades Using the Transient Liquid Crystal Technique,* ASME 94-GT-172.

[11] Whitaker, S., 1977, *Fundamental Principles of Heat Transfer,* Pergamon Press.

[12] Jones, T. V., 1991, *Definition of Heat Transfer Coefficient in the Turbine Situation,* IMECHE Paper C423/046.

[13] Turner, A. B., Tarada, F. H. A., and Bailey, F. J., 1985, *Effects of Surface Roughness on Heat Transfer to Gas Turbine Blades,* AGARD-CP-390.

[14] Bown, N. W., Cain, T. M., Jones, T. V., Shipley, P. P., and Barry, B., 1994, *In Flight Heat Transfer Measurements on an Aero-Engine Nacelle,* ASME 94-GT-244.

[15] Kays, W. M. and Crawford, M. E., 1993, *Convective Heat and Mass Transfer,* McGraw Hill.

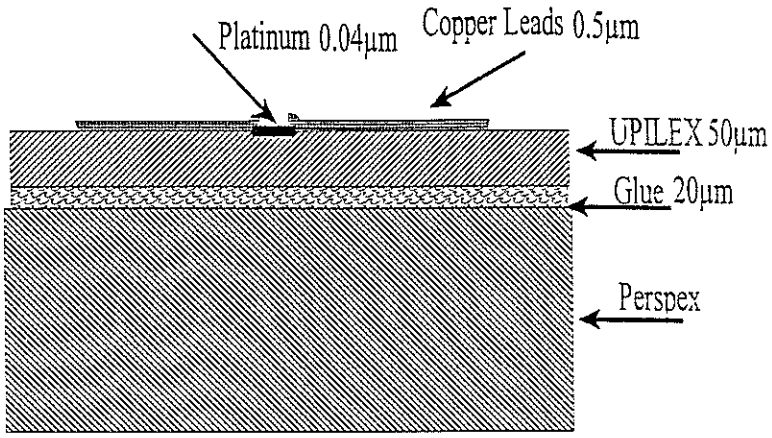

Figure 1: Schematic diagram of the thin film gauge

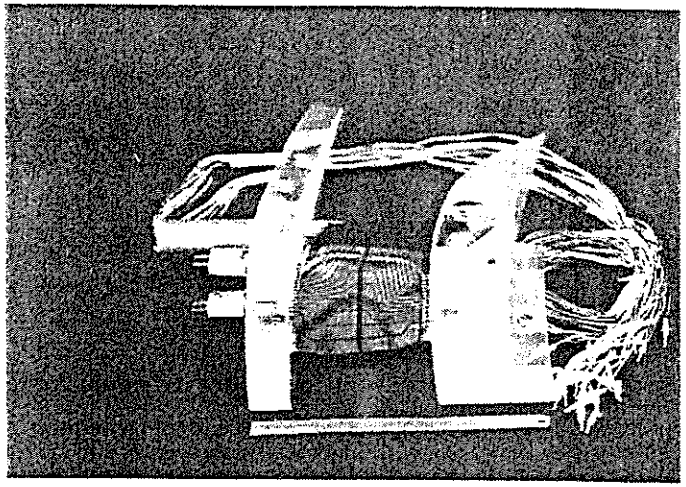

Figure 2a: Thin film gauges on the suction surface

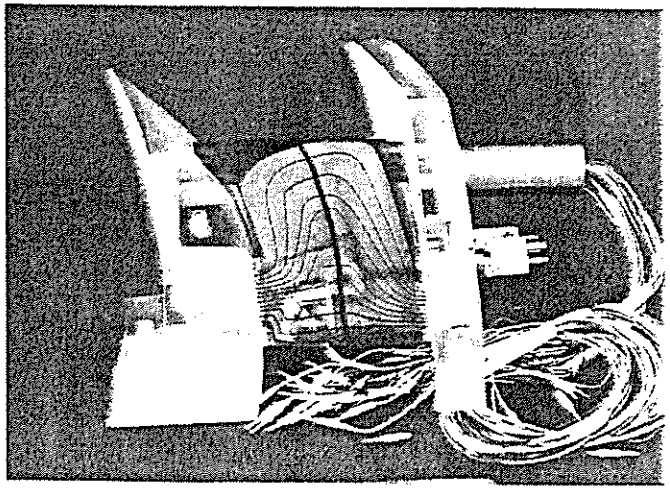

Figure 2b: Thin film gauges on the pressure surface

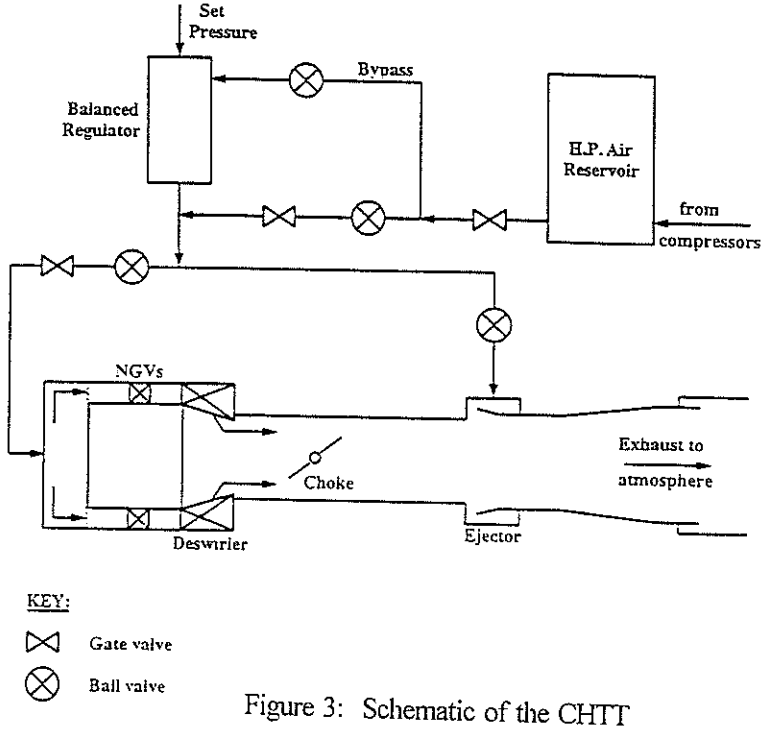

Figure 3: Schematic of the CHTT

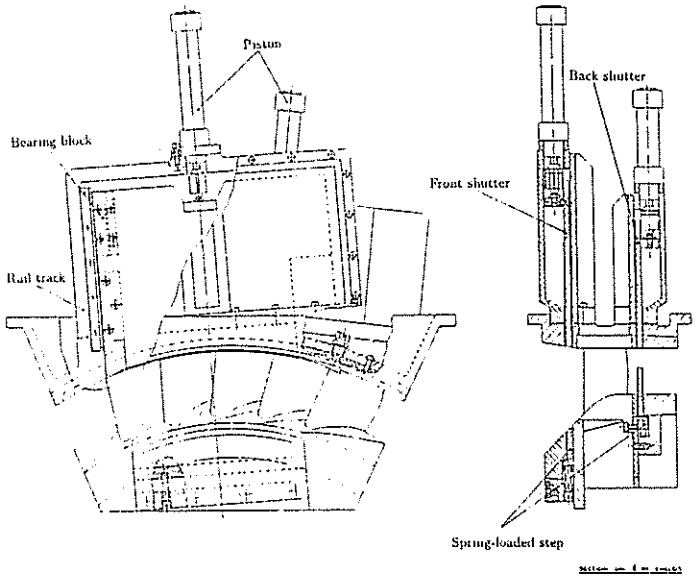

Figure 4: Heat transfer cassette

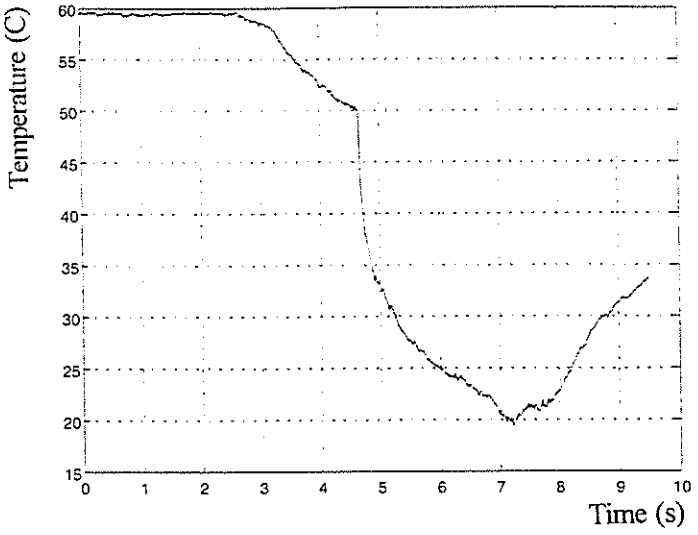

Figure 5a: Surface temperature history

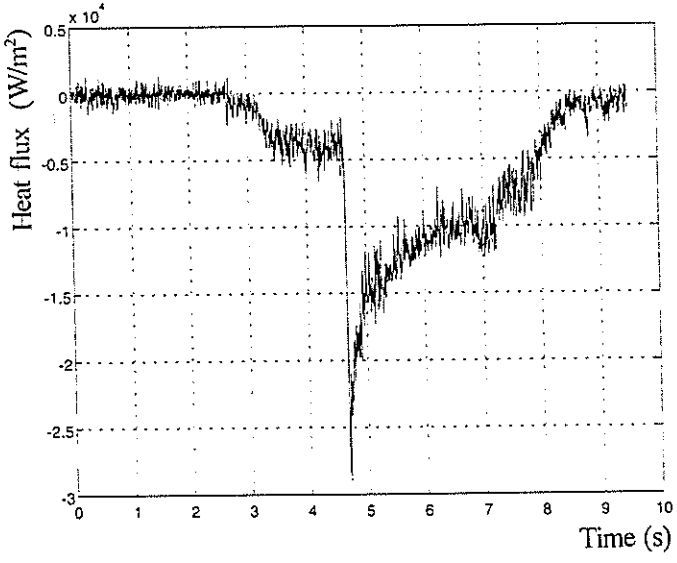

Figure 5b: Surface heat flux history

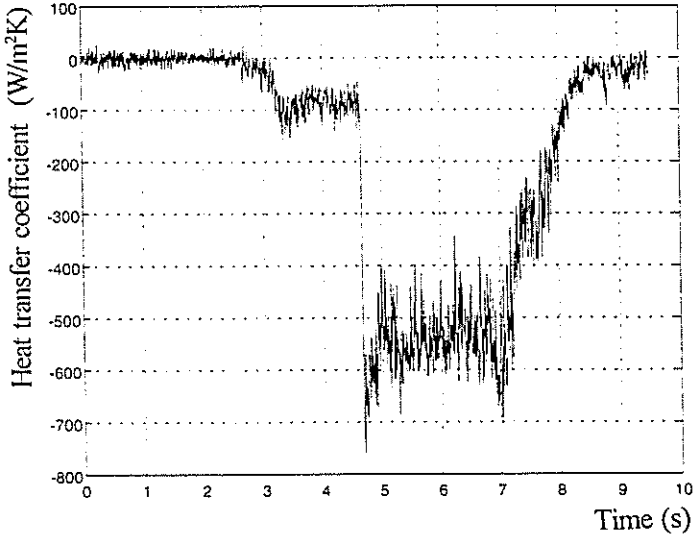

Figure 5c: Heat transfer history

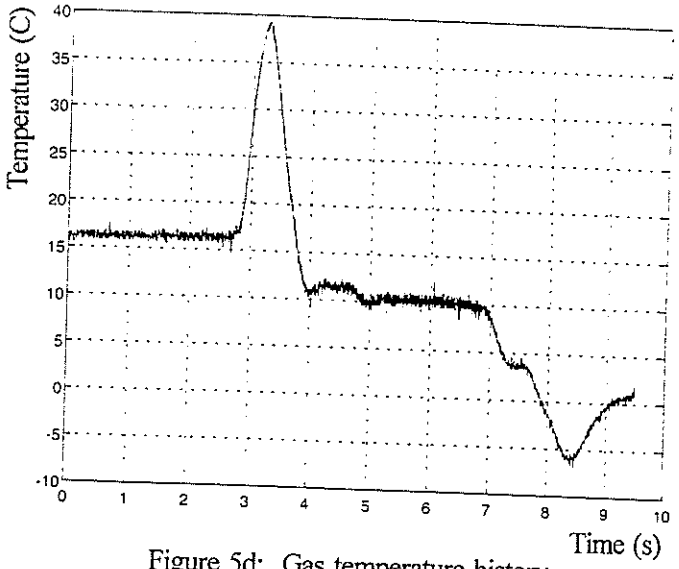

Figure 5d: Gas temperature history

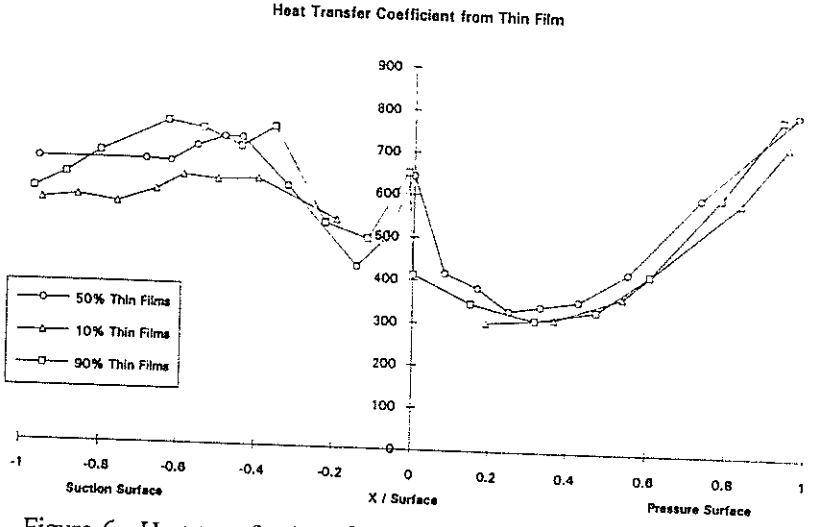

Figure 6: Heat transfer (W/m^2K) from the thin film gauges on perspex

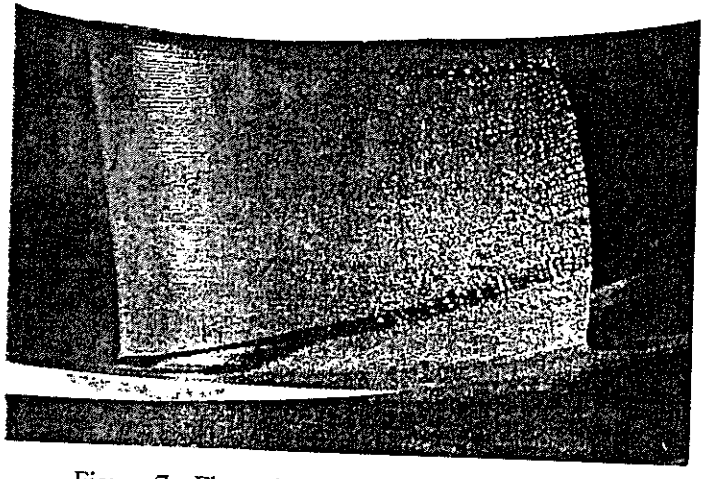

Figure 7: Flow visualization on the suction surface (100% span at bottom, flow left to right)

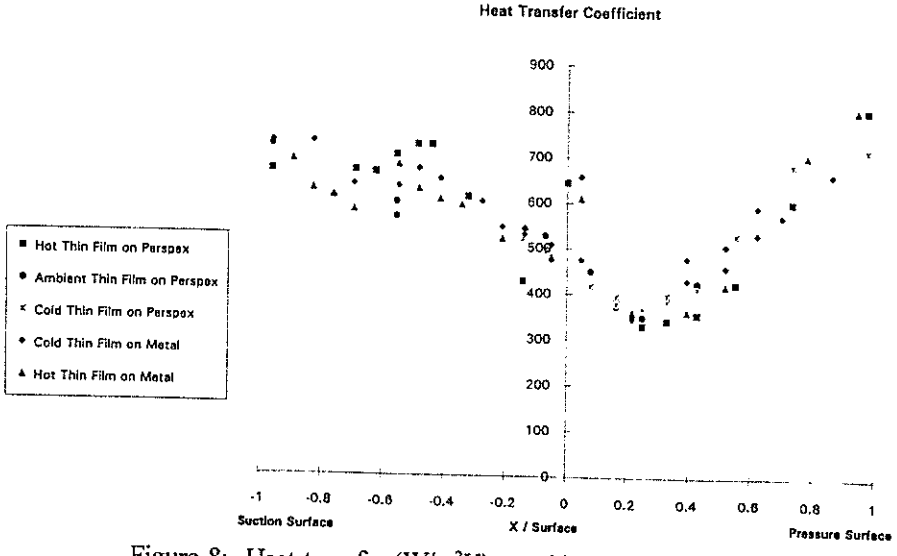

Figure 8: Heat transfer (W/m^2K) at midspan with different NGV materials and thermal boundary conditions

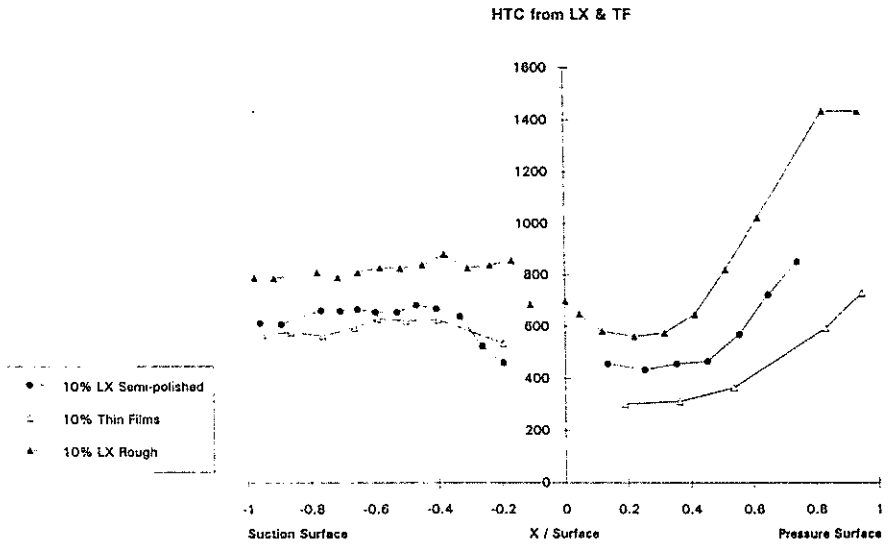

Figure 9: Heat transfer (W/m²K) from both thin film gauges and liquid crystal at 10% span

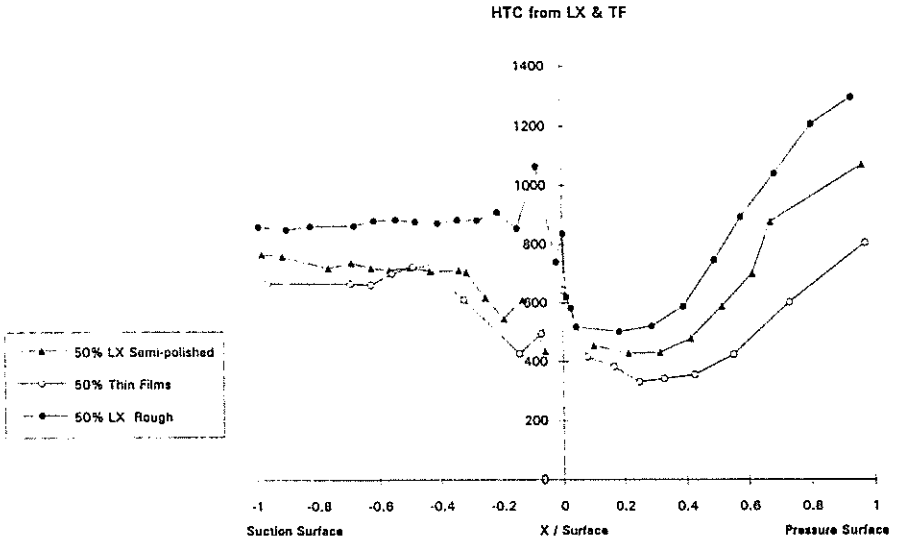

Figure 10: Heat transfer (W/m²K) from both thin film gauges and liquid crystal at 50% span

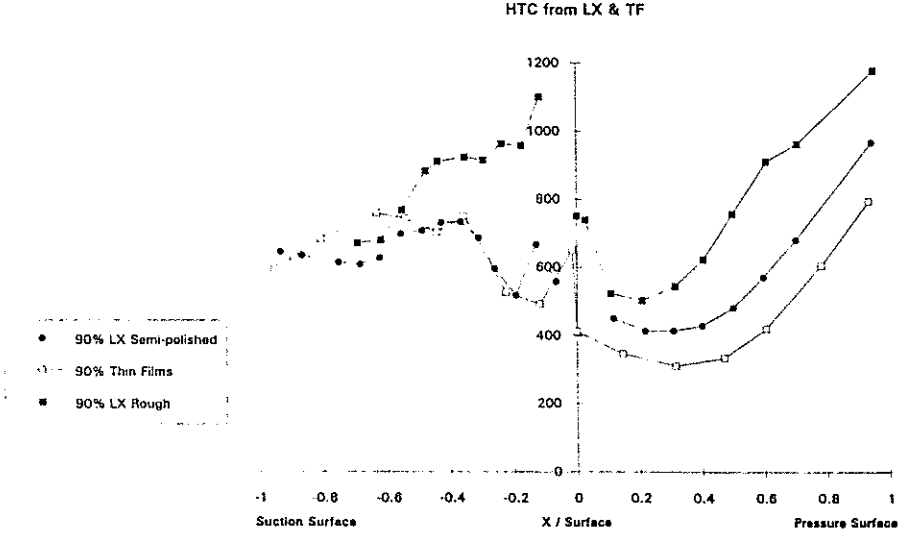

Figure 11: Heat transfer (W/m²K) from both thin film gauges and liquid crystal at 90% span

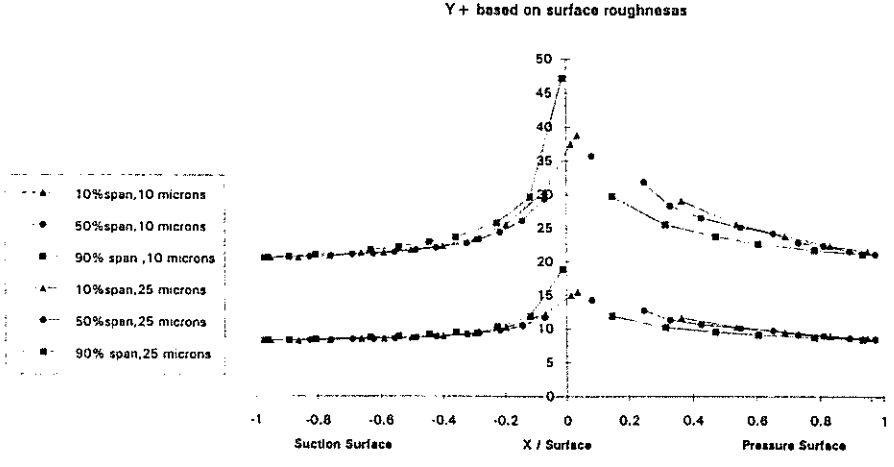

Figure 12: Roughness parameter along the NGV surface